Int. J. Electrochem. Sci., 11 **(2016)** 9282 – 9294, doi: 10.20964/2016.11.64

International Journal of
ELECTROCHEMICAL
SCIENCE
www.electrochemsci.org

Effect of Cu and Heat Treatment on the Corrosion Behaviour of a NiTi Alloy in Simulated Human Fluids

F. Salgado[1], *R. Lopez-Sesenes*[2], *I. Rosales*[1], *J.G. Gonzalez-Rodriguez*[1,*]

[1] Universidad Autonoma del Estado de Morelos, CIICAp, Av. Universidad 1001, 62209, Cuernavaca, Mor., Mexico.
[2] Universidad Autonoma del Estado de Morelos, Facultad de Ciencias Quimicas e Ingenieria, Av. Universidad 1001, 62209, Cuernavaca, Mor., Mexico.
[*]E-mail: ggonzalez@uaem.mx

Received: 3 August 2016 / *Accepted:* 16 September 2016 / *Published:* 10 October 2016

The effect of copper contents (5 and 10 at. %) and heat treatment (800^0C, 30 minutes) on the corrosion behavior of 45 (at.%)Ni-55Ti alloys in Hank´s solution has been studied by using potentiodynamic polarization curves and electrochemical impedance spectroscopy (EIS) measurements. Results have shown that both, the addition of Cu and heat treating the alloys increased the corrosion resistance of the base NiTi alloy. EIS measurements showed the existence of a duplex passive layer which was reinforced with the addition of copper or the heat treatment.

Keywords: NiTi alloys, Hank solution, Corrosion.

1. INTRODUCTION

Nickel-titanium (NiTi) alloys are widely used for orthopedic and dental application due to their super-elastic properties, shape memory effects, biocompatibility, good corrosion resistance, low density and strong enough[1-4]. These properties normally have been attributed to the titanium oxide (TiO_2) layer spontaneously formed on to the alloy surface[5-7]. According to literature [8-12] the high corrosion resistance of these alloys is due to a dense layer of TiO_2 which has a duplex structure, with an inner compact layer which acts as a barrier against the ion dissolution, so that the corrosion resistance increase with its thickness. There is also an outer porous layer, which is less corrosion resistance, but the incorporation of components from the electrolyte into its pores favors osteo-integration [13-15]. However, despite of its high corrosion resistance, the major concern of Ni-Ti alloys is the release of allergenic and toxic Ni^{2+} ions due to its corrosion for the human body fluids. To

prevent Ni dissolution, Ni-Ti alloys have been modified by using different surface treatments [16, 17]. The susceptibility of the Ni-Ti alloys to suffer rejection from human cells is now days an important issue to be resolved due to the high number of infections in patients that experiment this problems. Therefore, the objective to introduce a little amount of copper into the NiTi alloys is due to the need to improve the material acceptation in the human body since it is well known that cooper possesses excellent behavior as antiseptic and antibacterial material [18]. In this study, the effect of Cu concentration (5 and 10 at. %) as well as heat treatment on the corrosion behavior of a NiTi alloy will be evaluated in the Hank´s solution by using electrochemical techniques.

2. EXPERIMENTAL PROCEDURE

2.1 Testing material

Material tested in this study was a 45% at. Ni-55Ti base alloy with the addition of 5 and 10 at.% Cu. Alloys with nominal high purity Ni-Ti -Cu elements(99.98%) were fabricated by induction melting technique. In order to obtain lower amount of impurities a quartz crucible was used for melt the alloys inside of a chamber under vacuum atmosphere (10^{-3} Torrs). Alloys with Cu additions were heat annealed at 800^0C during 30 minutes under an Ar atmosphere. Heat treated specimens have been designated as HT. After reach the liquid state, the alloys were cooling down up to reach the solid state in the same crucible.

2.2 Corrosion tests

Electrolytic solution chosen for these experiments was the Hank´s solution with a chemical composition as given in table 1. For the corrosion evaluation in the Hank´s solution, potantiodynamic polarization curves and electrochemical impedance spectroscopy measurements were used.

Table 1. Chemical composition of Hank´s solution (g/L).

NaCl	$CaCl_2$	KCl	Glucose	$NaHCO_3$	$MgCl_2.6H_2O$	$Na_2HPO_4.2H_2O$	KH_2PO_4	$MgSO_47H_2O$
8	0.14	0.4	1	0.35	1	0.06	0.06	0.06

This solution simulates the physiological media of the human body. To perform the corrosion tests, specimens of 5 x 5 x 3 mm were machined by an electro discharge machine, encapsulated in epoxy resin and then grinded with 600-grade SiC emery paper, rinsed and degreased with acetone. Corrosion tests were carried out in a potentiostat from ACM-Instruments. Potentiodynamic polarization curves were carried out by polarizing specimen from ± 500 mV, around the free corrosion potential, E_{corr}, at a scan rate of 1mV/s. The E_{corr} value was monitored during 30 minutes, until it was stable, before starting the experiments. All the potentials are referred with respect to a Saturated Calomel Electrode (SCE) , whereas the counter electrode was a graphite rode. Corrosion current, I_{corr},

were calculated by using linear Tafel extrapolation. Electrochemical impedance spectroscopy measurements (EIS) were carried out at the E_{corr} value by applying a signal with an amplitude of ±10 mV in a PC4 300 Gamry potentiostat, in an interval frequency 10 KHz-0.5 Hz obtaining 50 points per decade**.** All tests were carried out at 37 ^{0}C.

3. RESULTS AND DISCUSSION

3.1 Microstructures

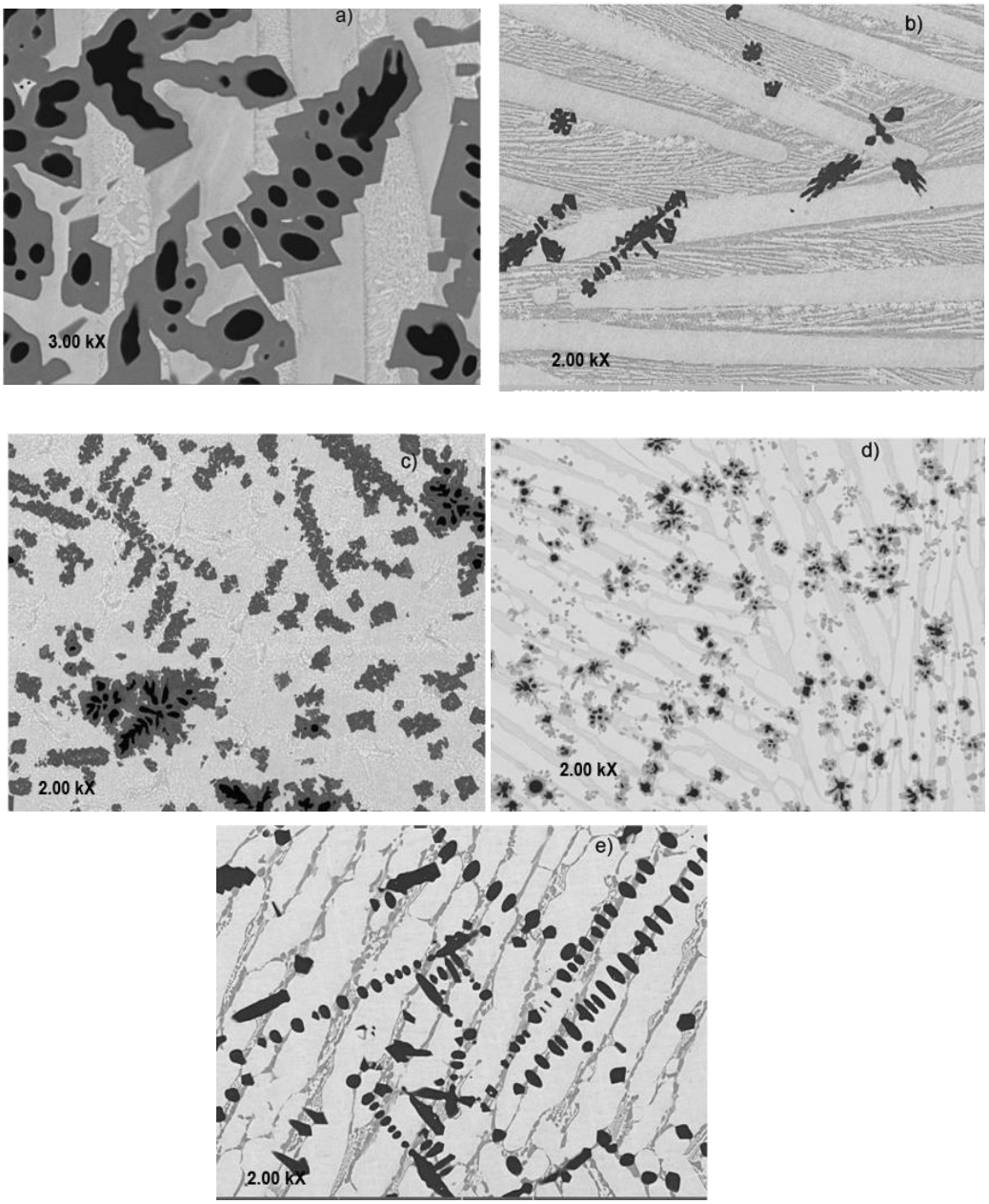

Figure 1. SEM micrographs showing the microstructures of a) 45Ni-55Ti, b) as-cast 45Ni-50Ti-5Cu, c) heat treated 45Ni-50Ti-5Cu d) as-cast 45Ni-45Ti-10Cu and e) heat treated 45Ni-45Ti-10Cu alloy.

SEM microstructures of the different tested materials are shown in Fig. 1. Fig. 1a show the image of the surface microstructure of the 45 Ni-55 Ti base alloy with the eutectic phase (grey zones) inside of columnar grains longer than 100µm can be seen. On the other hand, some dendritic structures are observed with a lower area fraction (dark zones). The differences in contrast is produced due to the differences in reflectivity depending of the phase orientation. The formation of $TiNi_3$ and Ti_2Ni is reported according to the alloy composition [19]. Microstructure of the sample 45Ni-50Ti-5Cu in as-cast condition is shown in Fig. 1 b, where columnar grains with an internal sub-nucleation of a second phase is observed. A lamellae eutectic structure grows with the same directions of the grains. Dark zones correspond to a dendritic phase precipitated on the alloy matrix. Fig. 1 c presents the image of the heat treated 45Ni-50Ti-5Cu alloy, where it can be observed that the columnar gran have been transformed and few equiaxed grains are formed due to the temperature effect; also, the lamellae eutectic structure it is not present any longer, presumably because it was dissolved into the alloy matrix. Some traces of dendritic structure are observed (black zones). The corresponding phases for this alloy with cooper additions correspond to Ti_2Ni, Ti_3Ni and Ti_2Cu. The surface microstructure of the alloy 45Ni-45Ti-10 Cu in the as-cast condition is presented in Fig. 1 d; at this copper concentration, big amount of small dendritic structures are observed of approximately 20 µm length, emerging from the alloy matrix which present a fine columnar grains. Finally, the surface microstructure of the heat treated 45Ni-45Ti-10Cu alloy is observed in Fig. 1 e, where it is notorious that columnar grains with larger size and some preferential orientation in comparison with the as cast condition. In the image is clearly visible that dendritic phase have considerably grown after the heat treatment. Ti_2Ni, Ti_3Ni and Ti_2Cu are the corresponding precipitated phases for these alloys with cooper additions in agreement with the ternary alloy phase diagram.

3.2 Polarization curves

Polarization curves for the different NiTi alloys in the Hank´s solution are given in Fig. 2, where it can be seen that all the alloys exhibit an active-passive behavior.

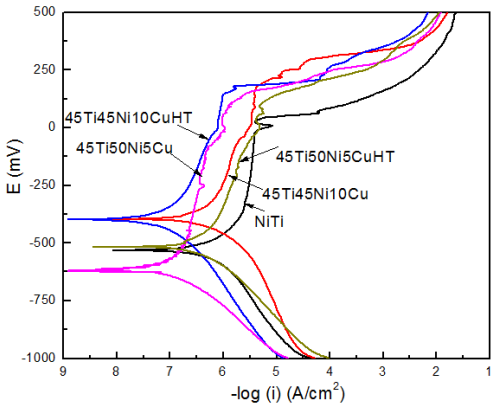

Figure 2. Effect of Cu contents and heat treatment on the polarization curves for Ni-Ti alloy in Hank´s solution.

Electrochemical parameters obtained from the polarization curves are shown in table 2. Base 45Ni-55Ti, the E_{corr} value is around -535 mV whereas the corrosion current density value, I_{corr}, was 1.6 x 10^{-6} A/cm^2. Polarization curves for the base alloy displays a passive zone which started approximately at a potential value close to -400 mV and ended in a pitting potential, E_{pit}, close to -20 mV. At this point, an abrupt increase in the current density can be observed due to the dissolution of the TiO_2 passive layer. [8-12] Passivation current density value, I_{pas}, was 4 x 10^{-6}A/cm^2.

Table 2. Electrochemical parameters obtained from polarization curves of NiTi alloys in Hank´s solution.

Alloy	E_{corr} (mV)	I_{corr} (A/cm^2)	E_{pit} (mV)	I_{pas} (A/cm^2)
45Ni55Ti	-535	1.6 x 10^{-6}	-20	4 x 10^{-6}
45Ni50Ti5Cu	-615	1.6 x 10^{-7}	105	3.1 x 10^{-7}
45Ni50Ti5CuHT	-515	5 x 10^{-7}	100	1.2 x 10^{-7}
45Ni45Ti10Cu	-400	6 x 10^{-7}	190	1.5 x 10^{-7}
45Ni45Ti10CuHT	-395	1.6 x 10^{-7}	150	3.1 x 10^{-7}

HT= heat treated alloy

These values are similar to those reported for a Ti6Al4V alloy coated with TiNi [6] and pure Ti [20] in Hank´s solution. As soon as 5% Cu is added, the E_{corr} value shifts towards nobler values, or towards more active values when 10% Cu is added. Additionally, the I_{corr} and I_{pas} values were decreased up to one order of magnitude with Cu additions, obtaining the lowest values with 5% Cu, as well as with the heat treated alloy containing 10% Cu. Finally, the pitting potential value, E_{pit}, was increased with the addition of Cu, obtaining the highest values with the addition of 10% Cu. This improvement in the passive layer parameters such as a decrease in the passive current density as well as in the increase in the pitting potential values with the addition of Cu may be due to the formation of cooper oxides and their incorporation in to the TiO_2 passive layer reinforcing it.

3.3 Electrochemical impedance spectroscopy

EIS results, in both Nyquist and Bode-phase formats for base 45Ni-55Ti alloy are given in Fig. 3. Nyquist diagrams, Fig. 3 a, show capacitive-like, depressed semicircles, with their centers in the real axis, and with their diameters decreasing as time elapses. When the experiments were performed at a lower frequency, the semicircles were better defined but the impedance values were within the same order of magnitude, indicating that the corrosion process is under charge transfer control.

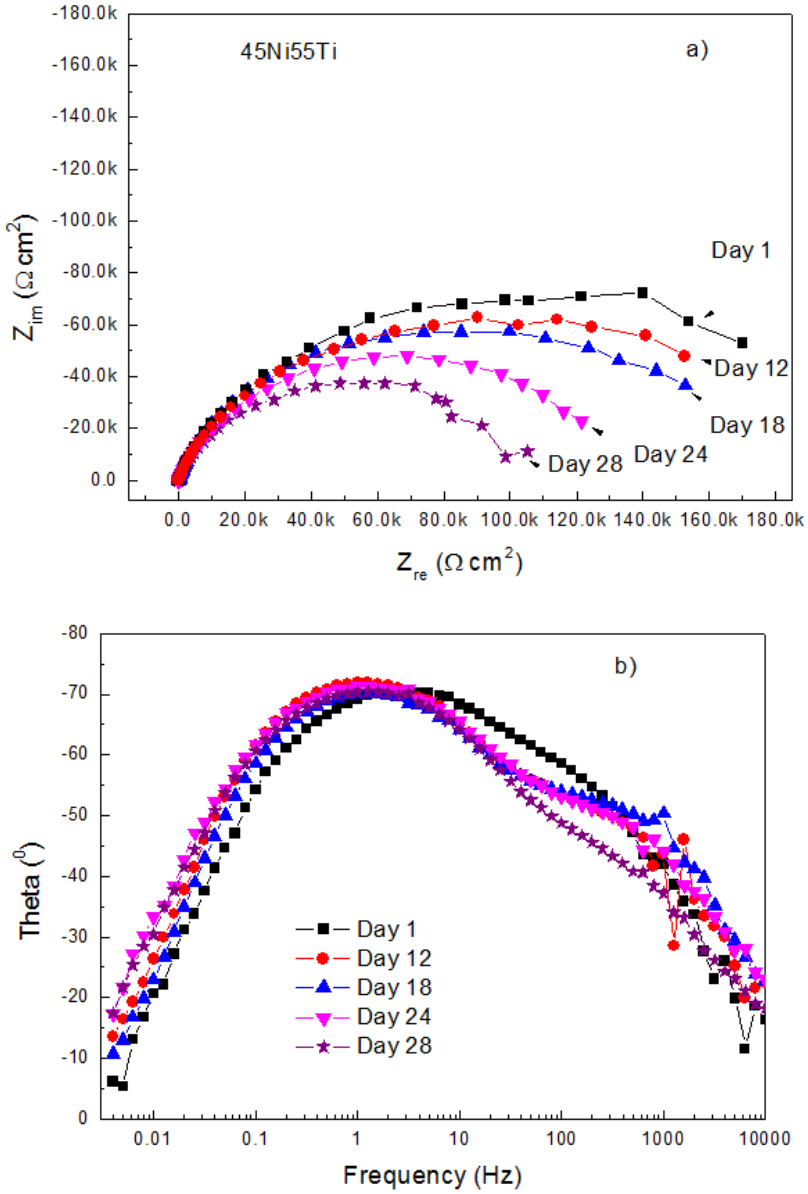

Figure 3. EIS data for 45Ni-55Ti alloy in Hank´s solution in the a) Nyquist and b) Bode-phase formats.

The fact that the real impedance values decrease as time elapses indicates an increase in the corrosion rate, due to a deterioration of the passive film. On the other hand, Bode diagrams, Fig. 3 b, clearly show two time constants, and according to the literature [8-12] the high corrosion resistance of these alloys is due to a dense porous layer of TiO_2 which has a duplex structure, with an external porous outer layer and an inner compact layer which acts as a barrier against the ion dissolution; thus, the two time constants correspond to these two layers. The corrosion resistance is attributed to the inner compact layer. Normally a passive material exhibit a highly capacitive behavior, where the phase angle remain constant, approaching 90^0, in a wide interval of frequencies, suggesting that a highly stable film is formed on tested alloy in the electrolyte used. In this case, phase angles during the first day of exposure is around 75^0, and it decreases as time elapses, indicating that the film on 45Ni-55Ti

alloys is not as stable as that reported for pure Ti alloy [20] and the film protectiveness decreases with time, as indicated by the decrease in the semicircles diameter observed in Fig. 3 a.

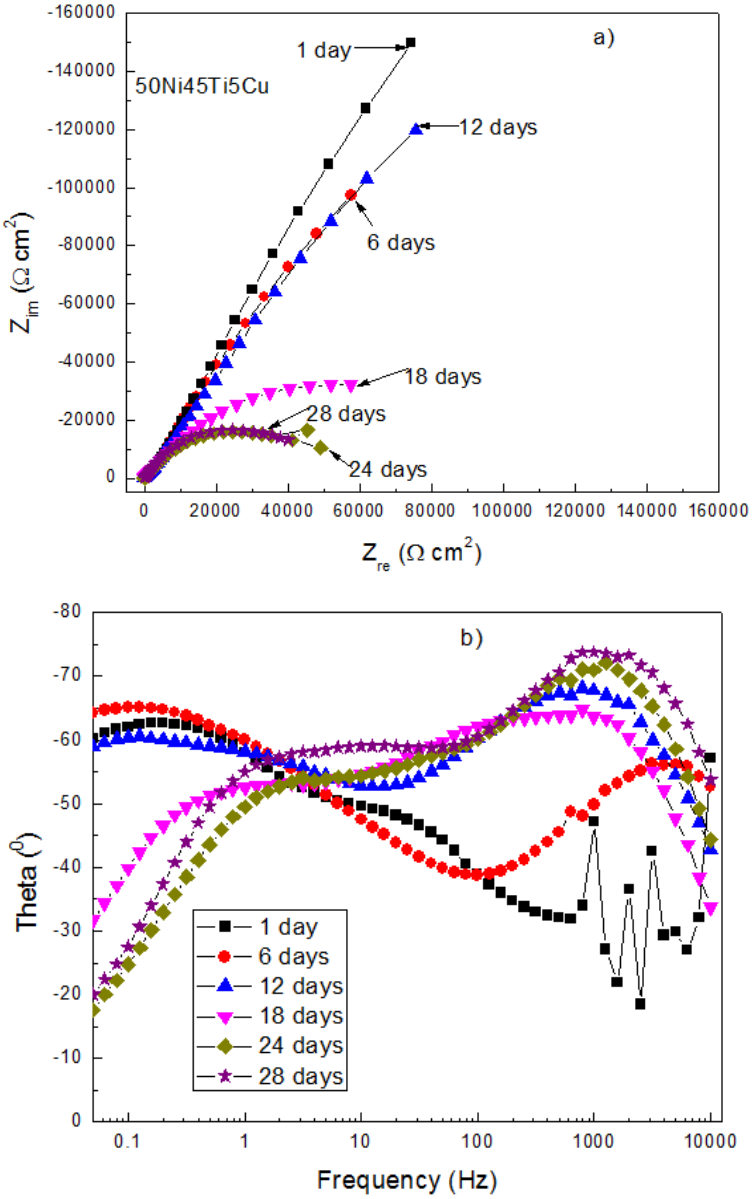

Figure 4. EIS data for the as-cast 45Ni-50Ti-5Cu alloy in Hank´s solution in the a) Nyquist and b) Bode-phase formats.

Nyquist and Bode-phase diagrams for the 45Ni-50Ti-5Cu alloy in the as-casting condition at different immersion times are given in Fig. 4. It can be seen that Nyquist diagrams, Fig. 4 a, display a single capacitive-like, depressed semicircle with its center in the real axis, indicating a charge transfer corrosion process. The semicircle diameter decreases as time elapses, indicating an increase in the corrosion rate as time elapses probably due to the penetration of the electrolyte though small film defects during exposure time. The impedance values for the 45Ni-50Ti-5Cu alloy are higher for those corresponding to the base 45Ni-55Ti alloy, which is more evident for the data at 28 days of immersion. The impedance for the base alloy after 28 days of exposure to the corrosive environment was around

27,500 ohm cm^2, whereas that for the 45Ni-50Ti-5Cu alloys was 40, 000 ohm cm^2, indicating a more protective passive film and a decrease in the corrosion rate due to the presence of Cu. On the other hand, Bode-phase diagrams, Fig. 4 b, show the presence of two time constants, which was not very clear during the first day of exposure, but it was more evident for longer exposure times. Phase angle at high frequency values increase with time, but at low frequency values decreases. This decrease in the phase angle, together with the decrease in the semicircle diameter, Fig. 4 a, indicates the decrease in the film protectiveness due to the penetration of the electrolyte through the film defects.

When the 45 Ni-50 Ti-5 Cu alloy was heat treated, Fig. 5, Nyquist diagrams displayed depressed, capacitive-like semicircles, but its diameter sometimes increased and some others decreased as time elapsed, indicating an unstable the passive formed film on the alloy. The increase in the total impedance indicates an improvement on the film protectiveness, due to an increase in its thickness, and a decrease in the total impedance indicates a decrease in the film thickness due its dissolution or to its disruption.

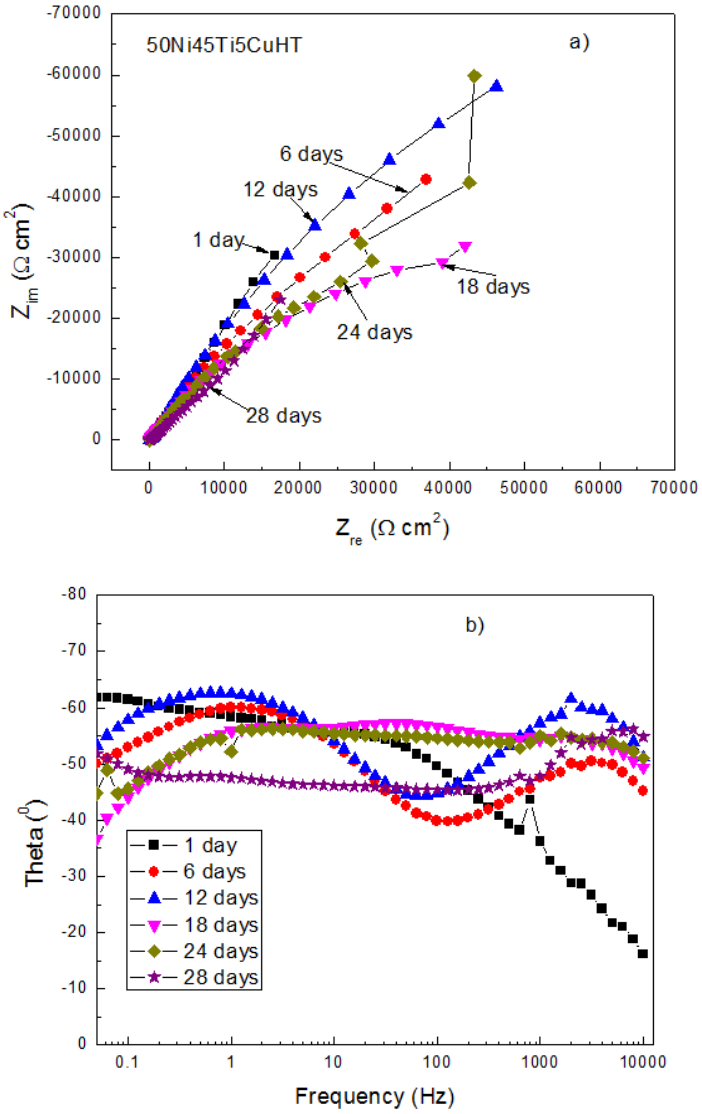

Figure 5. EIS data for the heat treated 45Ni-50Ti-5Cu alloy in Hank´s solution in the a) Nyquist and b) Bode-phase formats.

This might be due to the fact that for the heat treated alloy, the amount of dendritic phases inside the equiaxed grains is much higher than that for the as-casting alloy, Fig. 1, increasing the number of sites where the passive film can be disrupted. Bode-phase diagrams, Fig. 5 b, showed the presence of two time constants, and the phase angle sometimes increased and some others decreased as time elapsed for the reasons given above. However, the phase angle value were lower than those for the same alloy but without heat treatment, indicating a much lower corrosion resistance of the former, due to the electrolyte penetration and to the film disruption.

EIS diagrams for the as-cast 45Ni-45Ti-10Cu alloy are given in Fig. 6. Nyquist diagrams, Fig. 6 a, show a single capacitive-like, depressed semicircle at all frequency values, with its diameters decreasing with an increase in time. This fact indicates that the corrosion process is under charge control, indicating an increase in the corrosion rate as time elapses due to the penetration of the electrolyte trough the film defects.

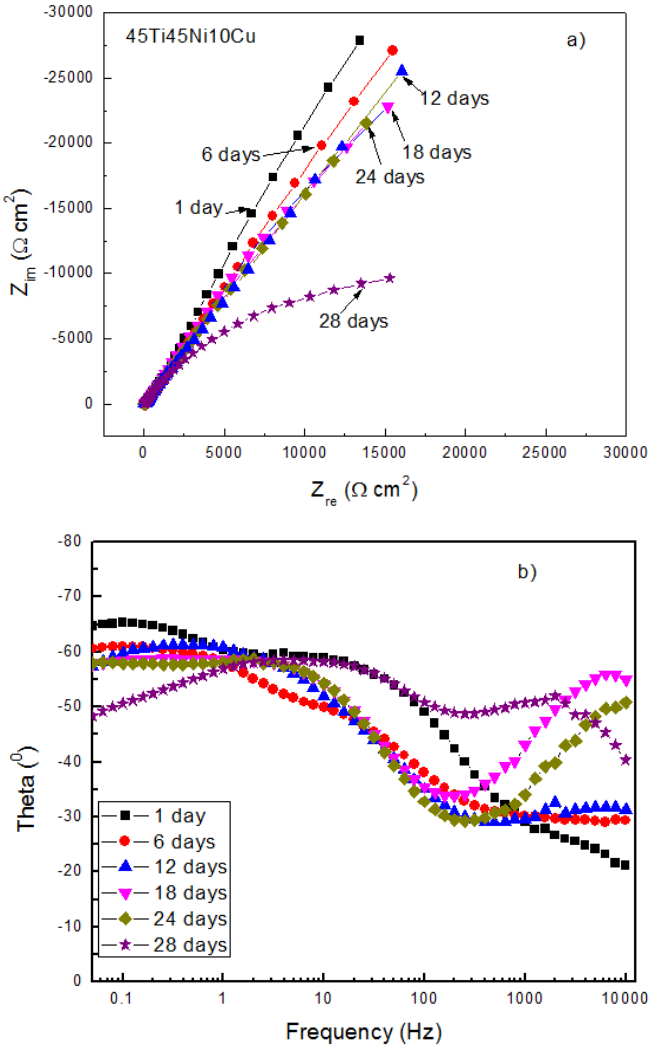

Figure 6. EIS data for the as-cast 45Ni-45Ti-10Cu alloy in Hank´s solution in the a) Nyquist and b) Bode-phase formats.

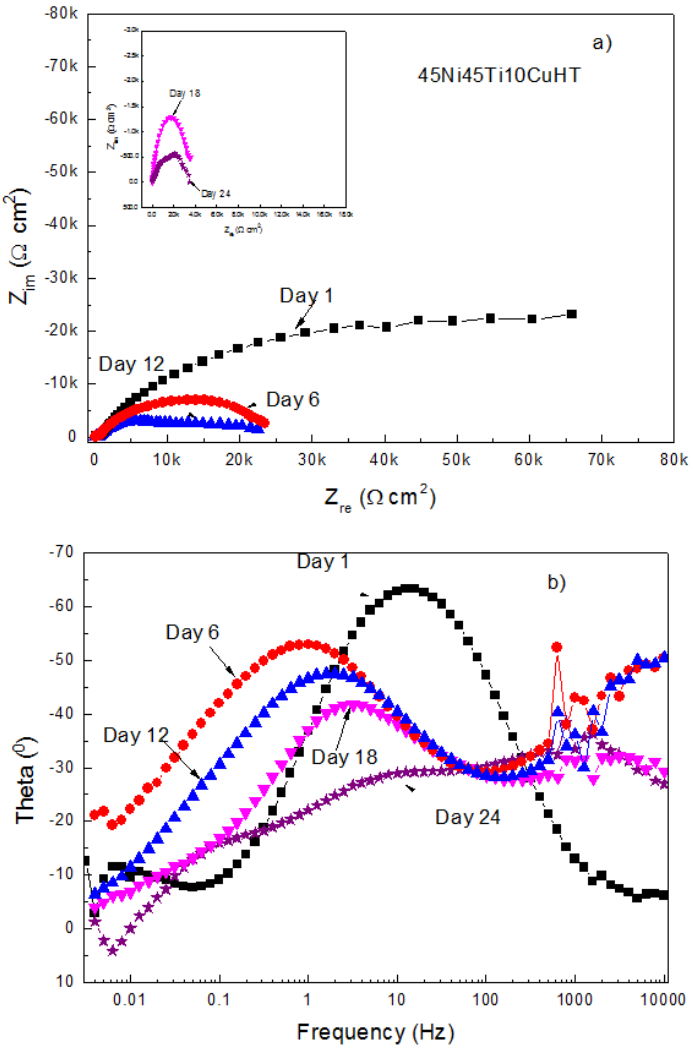

Figure 7. EIS data for the heat treated 45Ni-45Ti-10Cu alloy in Hank´s solution in the a) Nyquist and b) Bode-phase formats.

Bode-phase diagrams, Fig. 6 b, show two time constants, with a decrease in the phase angle as time elapses, due to the penetration of the film by the electrolyte and an increase in the corrosion rate. For heat treated 45Ni-45Ti-10Cu alloy, Fig. 7, Nyquist diagrams also displayed capacitive semicircles at all frequency values, and its diameter decreased as time elapsed during the whole experiment increasing, thus, the corrosion rate. The total impedance values were higher than those for the as cast 45Ni-45Ti-10Cu alloy, which indicates a higher corrosion resistance for the former as indicated in polarization curves, Fig. 2**.** Bode-phase diagrams, Fig. 7 b, show a wide peak around -65^0 during the first day of exposure to the electrolyte, indicating a very stable passive film on top of the alloy. The frequency interval where the phase angle peak is constant decreases during the rest of the experiment, which indicates a decrease in the passive film protectiveness, and thus, an increase in the corrosion rate. With a further increase in the exposure time, the frequency interval where the phase angle peak remains constant increases once again, decreasing the corrosion rate of the alloy.

In order to simulate EIS data for the different tested alloys, electric circuit shown in Fig. 8 was used, as proposed by other authors [9-12, 21,22], which is composed by two layers, an external porous

outer layer and an inner barrier layer. In this circuits, R_s is the solution resistance, the resistance and admittance of the porous layer are R_p and Y_p respectively, whereas the resistance and admittance of the barrier layer are represented by R_b and Y_b are. Finally, n_b and n_p are parameters which indicate the deviation from a pure capacitive behavior [23].

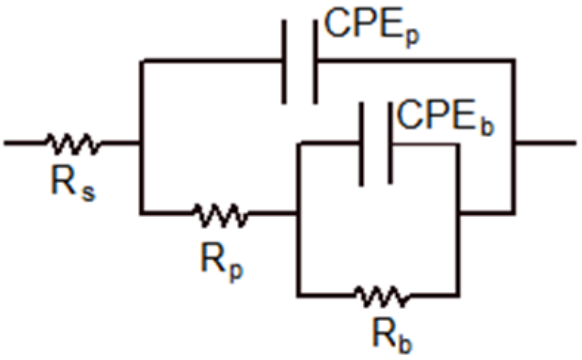

Figure 8. Equivalent electric circuit used to simulate the EIS data for NiTi alloys in Hank´s solution.

Table 3. Electrochemical parameters used to simulate EIS data of NiTi alloys after 1 day of exposure to the Hank´s solution.

Alloy	R_s (Ω cm^2)	CPE_p		R_p(Ω cm^2)	CPE_b		R_b (Ω cm^2) x 10^5
		Y_p (Ω^{-1} s^n) x 10^{-6}	n_p		Y_d (Ω^{-1} s^n) x 10^{-6}	n	
45Ni55Ti	1.83	9.5	0.83	1047	64	0.41	2.4
45Ni55Ti5Cu	1.61	13	0.71	10260	2.5	0.81	9.8
45Ni55Ti5Cu HT	1.77	50	0.67	291	47	0.65	4.8
45Ni55Ti10Cu	2.27	54	0.72	11121	62	0.75	5.4
45Ni55Ti10Cu HT	1.86	3.1	0.93	65	54	0.72	8.8

Parameters used to fit EIS data for the different NiTi alloys after 1 day of exposure to the Hank´s solution are given in table 3, where it can be seen that, irrespective of the chemical composition or heat treatment, the inner barrier layer resistance, R_b, is higher than that for the outer porous layer resistance, R_p, which supports the idea that the inner layer of the passive film determines the alloy corrosion resistance [24]. The highest R_b value is for the alloys containing 5% Cu and the heat treated alloy containing 10% Cu alloys, suggesting, thus, that these alloys have a higher corrosion resistance than the rest of the alloys, as evidenced by polarization curves in Fig. 2 and table 2. The lowest R_b value was for the base 45Ni55Ti alloy, which showed the highest corrosion resistance. From

table 2 we can see that for 45Ni55Ti alloy, the capacitance values, C, for the porous and inner layers are in the order of 10^{-6} and 10^{-5} F/cm^2 respectively. Nominally, the thickness of an oxide layer, δ, can be calculated by using following expression:

$$\delta = (\varepsilon\varepsilon_o A)/C \quad (2)$$

where ε and ε_o are the dielectric constants for the oxide and vacuum (8.85 x 10^{-12} F/m) and A the effective surface area [9]. Capacitance values can be calculated with following equation [9, 24]:

$$C = (Y_0 R^{-(n-1)})^{1/n} \quad (3)$$

We can see that the inner layer is thinner than the outer porous layer, but it offers more corrosion resistance. For alloy containing 5% Cu and heat treated 10% Cu alloys which offered the highest corrosion resistance, the inner layers were thicker and more compact than the outer porous layer, may be due to the formation of cooper oxides and their incorporation in to the TiO_2 passive layer, which gives more protection against the diffusion of the electrolyte. The fact that the from all the tested alloys, the lowest Y_b values was for the alloy containing 5% Cu, from eq. (2) is concluded that this is the thickest inner layer supports the idea that this thickening is due probably to the incorporation of copper oxide into this inner layer. The base 45Ni55Ti alloy, which has the highest Y_b value, would have the thinnest inner layer, and, thus, the lowest corrosion resistance. Due to a thicker and more compact inner layer in these alloys, slower diffusion processes appear on these alloys, which are the rate controlling step. The n_b values were in all cases either similar or lower than those for n_p, indicating a less capacitive behavior of the inner layer, suggesting that the mass diffusion through the inner layer is the rate controlling step [22, 25]. Only the heat treated alloy containing 10% Cu had an n value close to 1.0 (0.93) for the porous layer, indicating a nearly ideal capacitive behavior, resulting in a highly corrosion resistant alloy according to table 2. For this alloy, the porous layer was thicker than the inner layer, probably due to the incorporation of the electrolyte components into the pores of the outer porous layer, resulting in an increased corrosion resistant of this oxide layer.

4. CONCLUSIONS

A study on the effect of heat treatment as well as the addition of 5 and 10 at. % Cu on the corrosion resistance of a 45Ni-55Ti alloy has been carried out. Polarization curves have shown that the corrosion resistance was increased by adding either 5 or 10 % of Cu as well as by annealing the specimens at 800 ^{0}C for up to one order of magnitude due to the existence of a passive layer. Passivation current density values were also decreased whereas the pitting potential values increased. EIS measurements indicated that the passive layer was formed by an external porous layer and an inner, compact, which is the one which confers the corrosion resistance to the passive layer. It is thought that the addition of Cu to the alloy forms oxides which are incorporated into the passive layer reinforcing its corrosion resistance.

References

1. N.B. Morgan, *Mater. Sci. Eng., 378A*(2004)16.
2. S.A. Shabalovskaya, *Bio-Med. Mater.Eng*., 6(1996)267.

3. S.A. Shabalovskaya, *Biomed. Mater. Eng*., 12(2002)69.
4. C.W. Chan, H.C. Man, T.M. Yue, *Corrosi. Sci*., 56(2012)158.
5. N. A. Al-Mobarak , A. A. Al-Swayih, F. A. Al-Rashoud, *Int. J. Electrochem. Sci.*, *6*(2011)2031.
6. Bo Tian, Æ Dong, Bai Xie, Æ Fu, Hui Wan, *J. Appl. Electrochem.*, *39*(2009)447.
7. S. Gokul Lakshmi, S. Tamiselvi, N. Rajendran, D. Arivuoli, *J. Appl. Electrochem*., 34(2004)271.
8. S. Rao, T. Ushida, T. Tateishi, Y. Okazaki, S. Asao, *Biomed. Mater. Eng*., 6(1996)9.
9. S.L. Assis, S.O. Rogero, R.A. Antunes, A.F. Padilha, I. Costa, *J. Biomed. Mater. Res. B Appl. Biomater*., 73(2005)109.
10. E. Vasilescu, P. Drob, D. Raducanu, I. Cinca, D. Mareci, J.M. Calderon Moreno, M. Popa, C. Vasilescu, J.C. Mirza Rosca, *Corros. Sci.*, *51*(2009) 2885.
11. M.V. Popa, D. Raducanu, E. Vasilescu, P. Drob, D. Cojocaru, C. Vasilescu, S. Ivanescu, J.C. Mirza Rosca, *Mater. Corros*., 59(2008)919.
12. V.A. Alves, R.Q. Reis, I.C.B. Santos, D.G. Souza, T. de, F. Goncalves, M.A. Pereira da-Silva, A. Rossi, L.A. da Silva, *Corros. Sci*., 51(2009) 2473.
13. I.C. Lavos-Valereto, S. Wolynec, I. Ramires, A.C. Guastaldi, I. Costa, J. *Mater. Sci.: Mater. Med*., 15(2004)55.
14. J. Pan, H. Liao, C. Leygraf, D. Thierry, J. Li, *J. Biomed. Mater. Res*., 40(1998)244.
15. X. Liu, P.K. Chu, C.Ding , *Mater Sci Eng*., 471A(2004)49.
16. L.Mohan, D. Durgalakshmi , M. Geetha , T.S.N. Sankara Narayanan, R. Asokamani, *Ceram. Int*., 38(2012)3435.
17. V.A. Alves, R.Q. Reis, I.C.B. Santos, D.G. Souza, T. de F. Gonçalves, M.A. Pereira-da-Silva, A. Rossi, L.A. da Silva, *Corros. Sci*., 51(2009)2473.
18. X.B. Tian, Z.M. Wang, S.Q. Yang, Z.J. Luo, R.K.Y. Fu, P.K. Chu, *Surf. Coat. Technol*., 201(2007) 8606–8609.
19. M. Stearn, A.L. Geary, *J. Electrochem. Soc*. 105 (1958) 638-645.
20. N. A. Al-Mobarak, A. A. Ali, *Int. J. Electrochem. Sci*., 9 (2014) 32.
21. E. Vasilescu, P. Drob, D. Raducanu, I. Cinca, D. Mareci, J.M. Calderon Moreno, M. Popa, C. Vasilescu, J.C. Mirza Rosca, *Corros. Sci.*, *51*(2009)2885.
22. I. Milošev, M. Metikoš-Hukovic´, H.-H. Strehblow , *Biomaterials*, 21(2000)2103.
23. W. Wang, F. Mohammadi, A. Alfantazi, *Corros. Sci*. 57 (2012) 11–21.
24. S.L. Assis, I. Costa, *Mater. Corros*., 58(2007)329.
25. M. Metikoš-Hukovic´, A. Kwokal, J. Piljac, *Biomaterials*, 24(2003)3765.